# Output power smoothing of wind power plants using unified inter-phase power controller equipped with super-capacitor

Hajahmadi, Moahammad Ali ; Gharehpetian, Gevork B.; Firouzi, Mehdi ; Anvari-Moghaddam, Amjad; Blaabjerg, Frede

*Published in:*
Journal of Energy Storage

*DOI (link to publication from Publisher):*
10.1016/j.est.2022.105209



*Publication date:*
2022

*Document Version*
Accepted author manuscript, peer reviewed version

# Output Power Smoothing of WPPs Using UIPC Equipped with Super-Capacitor

M. A. Hajiahmadi[1], G. B. Gharehpetian[1], M. Firouzi[2], A. Anvari. Moghadam[3], F. Blaabjerg[3]
[1]Electrical Engineering Department, Amirkabir University of Technology, Tehran, Iran
[2]Department of Electrical Engineering, Abhar Branch, Islamic Azad University, Abhar, Iran
[3]Department of Energy Technology, Aalborg University, Aalborg, Denmark
E-mail: mymahaos@aut.ac.ir, grptian@aut.ac.ir, m.firouzi@abhariau.ac.ir, aam@et.aau.dk, fbl@et.aau.dk

*Abstract*- **Nowadays, by the growing attention to environmental and economic issues in power systems, the utilization of renewable energies, especially wind energy has increased. The inherent uncertainty of wind power plants (WPPs) output power is the main limiting factor for the integration of WPPs into power system. This paper presents the application of unified inter-phase power controller (UIPC) and the super-capacitor energy storage system (ESS) in smoothening output power of WPPs. To achieve this, a power control scheme is proposed to compensate the deviations between WPP output power and its reference set point. The WPP model studied here is of doubly-fed induction generator (DFIG) type wind turbine. To compare the performance of UIPC with and without ESS, a number of scenarios are examined in simulations in MATLAB/Simulink environment. The results demonstrate the effectiveness of the UIPC/ESS for smoothing output power and enhancing the low-voltage ride-through (LVRT) capability of WPPs.**

***Index Terms— Wind Power Plants (WPPs), Energy Storage System (ESS), Unified Inter-Phase Power Controller (UIPC), Super-capacitor (SC), Output Power Smoothing, Doubly-Fed Induction generator (DFIG)***

## I. INTRODUCTION

Nowadays, wind energy has developed far enough to become a worldwide considerable energy resource [1]. Numerous reports highlight that many countries around the globe have already set targets to meet an extensive amount of their electricity demand through wind power by 2030. For instance, US Department of Energy and European Wind Energy Association have set the goal of 20% and 22%, respectively[2]. Wind energy is an inexhaustible and pollution–free renewable energy resource (RES), however, the stochastic nature of this RES causes WPPs output power fluctuations, which introduces issues as follows [3-5]:

- Output power variations might lead to fluctuations in power system frequency, especially in weak isolated grids.
- Wind speed variations contribute to output power fluctuations of WPPs as well as their reactive power, which in turn may result in voltage flicker in power system.
- Both aforementioned problems (voltage flicker and frequency fluctuations) degrade the overall power quality of the system and may cause instability issues as well, especially to sensitive loads.

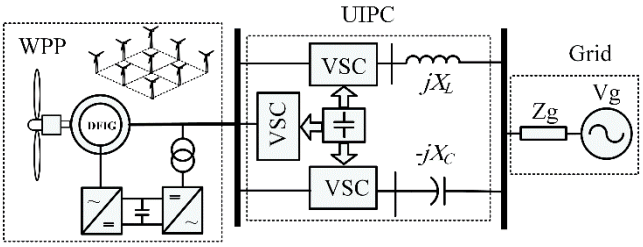


Fig. 1: Wind Power Plant connected to power system through UIPC

In the literature, several solutions have been proposed to smooth the fluctuations of WPPs output power, which can be classified into two main categories according to the presence of ESS [6]. One solution is to utilize the energy stored within wind generation system, including control of the kinetic energy [7-8], pitch angle [9-10], and DC link capacitor voltage [11]. Another alternative is to use ESSs such as superconducting magnetic energy storage (SMES)[12-13], super-capacitor (SC) [14-15], flywheel [16] and various types of batteries [17-19] in WPPs.

The ESS-based power smoothing technics have similar algorithms. There are two schemes for installation of ESSs in WPPs; One is to connect the ESS to the terminals of the WPP. This scheme requires a voltage source inverter (VSI), a step-down transformer, a buck-boost converter and a capacitor in DC link. Another scheme is to connect the ESS to the DC-link of the flexible AC transmission system (FACTS) controllers such as static synchronous compensator (STATCOM) [20-21], unified power flow controller (UPFC) [22] and static synchronous series compensator (SSSC) [23], which requires only a buck-boost converter.

In [25], utilization of UIPC is proposed to connect WPPs to power system, with purpose of controlling the WPPs output power as well as to limit the contribution of WPPs in fault currents, as depicted in Fig. 1. The UIPC configuration is based on the inter-phase power controller (IPC) [26-27]. However, the phase-shifting transformers in IPC are replaced by three voltage source converters (VSCs), which share a common capacitor in their DC side. UIPC is capable of controlling power flow under steady-state condition and limiting short circuit currents through voltage isolation under fault condition [28-29].

In [30], a modified UIPC has been developed for power flow control in a hybrid AC-DC microgrid. In [31], a damping controller has been designed and integrated into the UIPC control system with purpose of enhancing the transient stability of power system in presence of WPPs. Authors of [32] have utilized UIPC to improve the LVRT capability of WPP. It was recognized as an effective solution to overcome WPPs connection issues. In all of the aforementioned studies, the wind speed is considered constant, and no control scheme has been proposed for variable wind speed WPPs.

Considering the literature, this paper presents an output power smoothing scheme incorporating a UIPC and SC as storage. The UIPC equipped with ESS can control the power flow and provide a smooth power profile under variable wind speed. Moreover, integrating the ESS increases the UIPC capability to enhance the LVRT performance of WPPs. To achieve this, a supervisory control is designed to generate the outer control loop for the UIPC power regulation as well as the ESS control based on compensating the deviations between WPP output power and its reference value. Simulations are performed in MATLAB/Simulink environment on a DFIG-based WPP to evaluate the effectiveness of the proposed UIPC/ESS scheme.

## II. UIPC EQUIPPED WITH ESS

Fig. 2 (a) demonstrates the configuration of the UIPC/ESS, which is comprised of two shunt branches; inductive and capacitive. The inductive branch consists of a series inductor and series VSC (SEC1). Similarly, the capacitive branch consists of a series capacitor and series VSC (SEC2). Additionally, a shunt VSC (SHC) is used to provide SEC1 and SEC2 with the required active power. To smoothen the WPP output power, a SC is incorporated in the DC link as ESS. The UIPC is modeled as a voltage-controlled current source $I_U$, which can be expressed by the following equation [25]:

$$I_U = \frac{V_S}{X}\, sin(\alpha) \angle\ \beta \tag{1}$$

where, $\alpha = (\varphi_2 - \varphi_1)/2$, $\beta = (\varphi_2 + \varphi_1)/2$ and $X=X_L=X_C$. The UIPC active and reactive powers are written by [25]:

$$P_U = 2\frac{|V_s||V_r|}{X}\, sin(\alpha)\ cos(\delta + \beta) \tag{2}$$

$$Q_U = 2\frac{|V_s||V_r|}{X}\, sin(\alpha)\ sin(\delta + \beta) \tag{3}$$

From equations (2) and (3), the following can be derived.

$$S_U = \sqrt{{P_U}^2 + {Q_U}^2} = 2\frac{|V_s||V_r|}{X}\, sin(\alpha) \tag{4}$$

$$\frac{Q_U}{P_U} = \tan(\delta + \beta) \tag{5}$$

Equations (4) and (5) are used to obtain $\alpha$, and $\beta$ for each set of active and reactive power [25, 30-31].

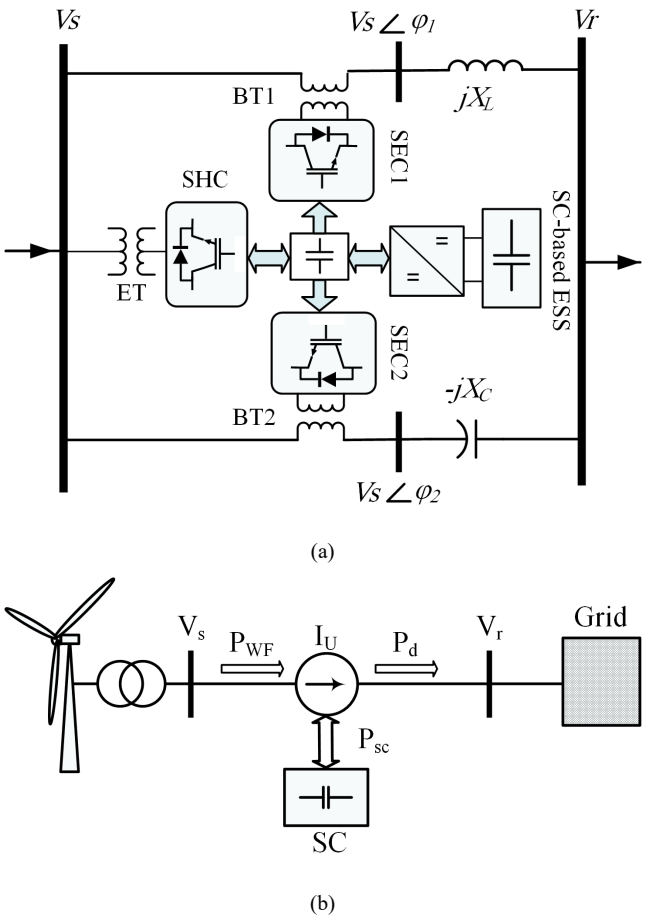


Fig. 2: Schematic diagram of (a) UIPC/ESS power circuit, (b) grid-connected WPP with UIPC/ESS

Fig. 2(b) demonstrates the grid connected WPP with the UIPC/ESS. The ESS consists of a SC and a bidirectional DC-DC buck/boost converter connected to the UIPC capacitor in its DC link. For the purpose of smoothening WPP power, if the ESS is applied to the WPP, it requires to be integrated at each DFIG DC link, hence making the control strategy of each DFIG and ESS complicated. Considering this problem and to simplify the smooth power control of WPPs, an SC-based ESS is incorporated into the DC link of the UIPC. Using the UPIC/ESS, all wind turbines can operate within their maximum power point, without any modifications in control system. Moreover, using the ESS enhances the power system transient conditions [21-22].

The ESS contributes to control the UIPC active power according to the reference value under variable wind speed. In Fig. 2 (b), $P_{WF}$, $P_d$ and $P_{sc}$ represent the WPP output power, output power reference, and active power exchange between the UIPC and ESS system, respectively. The main function of the UIPC/ESS is to control the WPP output active power according to output power reference ($P_d$). To achieve this, a UIPC supervisory control (USC) is designed to generate the outer-loop power controllers for the UIPC and ESS control. The USC is described by the flowchart diagram depicted in Fig. 3(a).

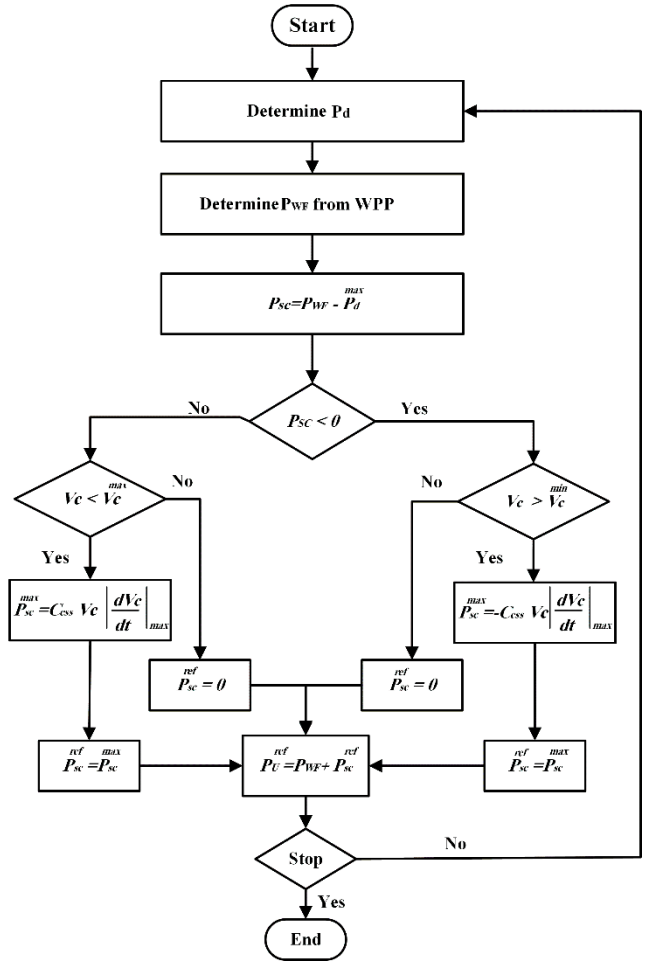


(a)

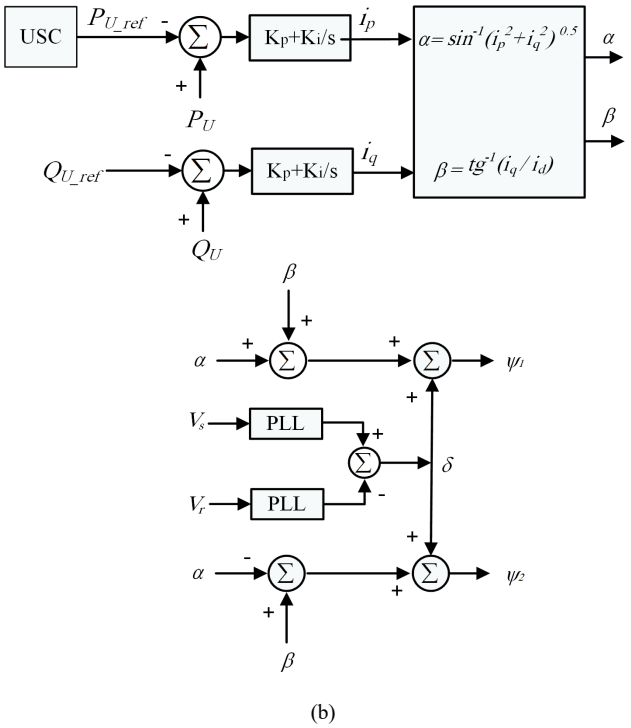


(b)

Fig. 3: (a) Flowchart diagram of USC and, (b) UIPC control system

To supply the output power reference, the difference between $P_d$ and $P_{WF}$ is injected or stored in the SC as follows:

$$P_{SC} = P_{WF} - P_d \tag{6}$$

On the other hand, the SC voltage ($V_C$) must satisfy the following inequality constraints:

$$V_C^{min} < V_C < V_C^{max} \tag{7}$$

where, $V_C^{max}$ and $V_C^{min}$ represent the maximum and minimum limits of the SC voltage, respectively. $P_{SC}^{max}$ is the maximum power exchanged between the SC and the UIPC DC link and is determined by:

$$P_{SC}^{max} = \pm\, C_{ess} V_C \left|\frac{dV_C}{dt}\right|_{max} \tag{8}$$

where, $\left|\frac{dV_C}{dt}\right|_{max}$ is the maximum rate of voltage variations of SC, and depends on the SC current limit. The positive and negative signs in equation (8) denote storing and suppling energy by the SC, respectively. Considering Fig. 3(a), the $P_{SC}^{ref}$ is subjected to $V_C^{max}$ and $V_C^{min}$. If $P_{SC}>0$, the SC charges by the DC link capacitor. In this case, if $V_C < V_C^{max}$, $P_{SC}^{ref}$ is calculated using (8), else $P_{SC}^{ref} = 0$, and the SC cannot store any power. Similarly, if $P_{SC}<0$, the SC discharges by the DC link capacitor. In this case, if $V_C > V_C^{min}$, $P_{SC}^{ref}$ is calculated using (8), else $P_{SC}^{ref} = 0$. By calculating $P_{SC}^{ref}$, the active power reference of the UIPC ($P_U^{ref}$) is determined as follows:

$$P_U^{ref} = P_{WF} + P_{SC}^{ref} \tag{9}$$

Fig. 3(b) presents the control system of UIPC according to the USC and equations (4) and (5). The control system of SHC system has been presented in [30-31].

## III. SC-BASED ESS

The SC is an electrochemical capacitor which has higher energy capacity compared to the conventional capacitors. This is due to employment of conducting polymers as the electrodes, thin dielectric and large surface area. The capacitance of the SC is expressed as follows [33]:

$$C_{ess} = \frac{2P_C^{max}T_C}{V_C^2} \tag{10}$$

where $P_C^{max}$, $T_C$ and $V_C$ represent the maximum stored active power, the time period for charging /discharging with $P_C^{max}$, and the rated SC voltage, respectively.

Fig. 4 demonstrates the control system for switches $S_1$ and $S_2$ of DC/DC converter to regulate the ESS output power. Considering $P_{sc}^{ref}$ provided by the USC, the DC/DC converter operation is classified into two modes as presented in Table I. If $P_{WF}<P_d$ ($i.e.\ P_{sc}^{ref} < 0$), the control system opens $S_1$ and the DC/DC converter operates in boost mode. In this mode, the SC supplies the active power to the UIPC

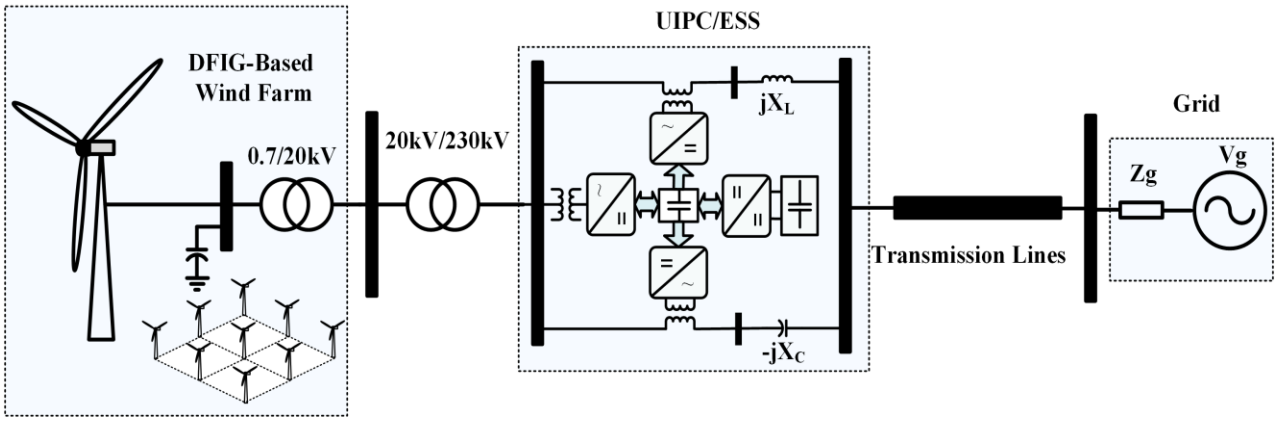


Fig. 5: Single line diagram of the study system with the UIPC/ESS

DC link. If the $P_{WF}>P_d$ $(i.e.\ P_{sc}^{ref} > 0)$, the control system opens $S_2$ and the DC/DC converter operates in buck mode and the SC absorbs the active power from the DC link.

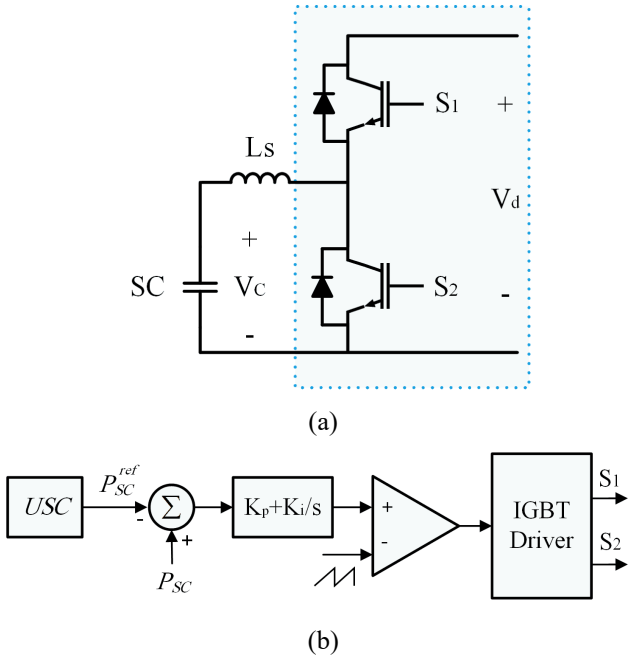


Fig. 4. Configuration of SC-based ESS (a) power circuit, (b) control system

Table. I. Operation modes of the DC-DC converter

| Condition | $S_1$ | $S_2$ | Operation Mode |
|---|---|---|---|
| $P_{ess}^{ref} < 0$ | open | $D_2$ | Boost |
| $P_{ess}^{ref} > 0$ | $D_1$ | Open | Buck |

## IV. Description of The WPP Model

The WPP simulated in this study is modelled by an equivalent aggregated DFIG, derived by an aggregated variable speed WT [34]. The two-mass model drive train is considered in this study to investigate the LVRT response of the DFIG-based WPP [35]. Fig. 5 demonstrates the single line diagram of the study WPP connected to grid through the UIPC/ESS. The simulated WPP consists of 60* 1.67 MW DFIG-based WTs. Here, the ESS is designed to absorb/inject 15% of the UIPC rated power (100 MVA) for 20s. Simulations are performed to demonstrate the UIPC/ESS capability for smoothing output power under variable speed condition. The power reference is assumed to be 85 MW. Parameters of the UIPC and the system under study are presented in Table II.

Table II: Simulation Parameters

| **DFIG** | | **UIPC** | |
|---|---|---|---|
| **Parameter** | **Value** | **Parameter** | **Value** |
| Rated Power | 1.67 MW | Rated SEC1 and 2 | 50MVA |
| Number of Blades | 3 | AC Voltage | 230kV |
| Inertia Constant | 1.432 s | DC Link Voltage | 40kV |
| Stator Voltage | 0.69 kV | $X_L$=$X_C$ | 120 Ω |
| Rotor Voltage | 2 kV | ESS Capacitor | 60 F |
| Nominal Frequency | 60 Hz | ESS Voltage | 4 kV |
| DC Voltage | 1150 V | **Test system** | |
| Stator Resistance | 0.023Ω | Source Voltage | 230kV |
| Stator Reactance | 0.18Ω | Nominal Power | 100MVA |
| Rotor Resistance | 0.016Ω | Line Resistance | 0.025Ω/km |
| Rotor Reactance | 0.16Ω | Line Inductance | 0.93mH/km |
| Capacitor | 5 mF | Line Capacitance | 0.012uF/km |

## V. Simulation

To investigate the Efficiency of the UIPC/ESS the system shown in Fig. 5 is considered. Firstly, output power smoothing capability of the WPP is examined using the UIPC/ESS. Afterwards, a three-line to ground (3LG) fault is simulated to investigate the LVRT capability of the UIPC/ESS. Following scenarios have been considered:

- Scenario A: Without using any UIPC
- Scenario B: Using the UIPC
- Scenario C: Using the UIPC/ESS

### A. Smoothing Output Power

In this section, the simulation time is considered to be 100s to investigate the UIPC/ESS performance under variable wind speed condition and for all three aforementioned scenarios:

Fig. 6 demonstrates the assumed and simulated wind speed profile, varying from 11.7 m/s to 14 m/s. Fig. 8 demonstrates the WPP output power for three scenarios. In scenario A, the WPP output power fluctuates in the range of 75-97 MW, as shown in Fig. 7(a). Using the UIPC in scenario B, the WPP output power fluctuations are reduced in the range of 70-88 MW as shown in Fig. 7(b). However, by using the UIPC/ESS in scenario C, the WPP output power is controlled in 87 MW according to power reference.

Fig. 8(a) and Fig. 8(b) demonstrate the output active power and voltage of super-capacitor ESS under variable speed, respectively. When the wind power generation is more than the calculated reference, the ESS stores extra power and vice versa as shown in Fig. 8(a). Fig. 9(a) and Fig. 9(b) depict the inductive and capacitive SECs injected voltage to control the WPP output power for all scenarios, according to the power reference. It can be observed from this figure that the inductive and capacitive SEC voltages are controlled in 0.38pu and 0.423pu in scenario C, respectively. However, they are varied according to wind speed variations in case of using UIPC in scenario B. Fig. 10(a) and Fig. 10(b) show the inductive and capacitive branches voltage phase angles to control the WPP output power for all scenarios. In scenario B, the phase angle of inductive branch vary in range of 32.5 to 32.8 degrees. However, it is controlled in 33.1 degrees in scenario C.

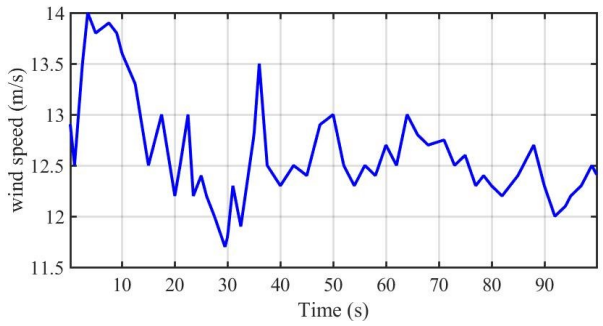


Fig. 6. Wind speed profile

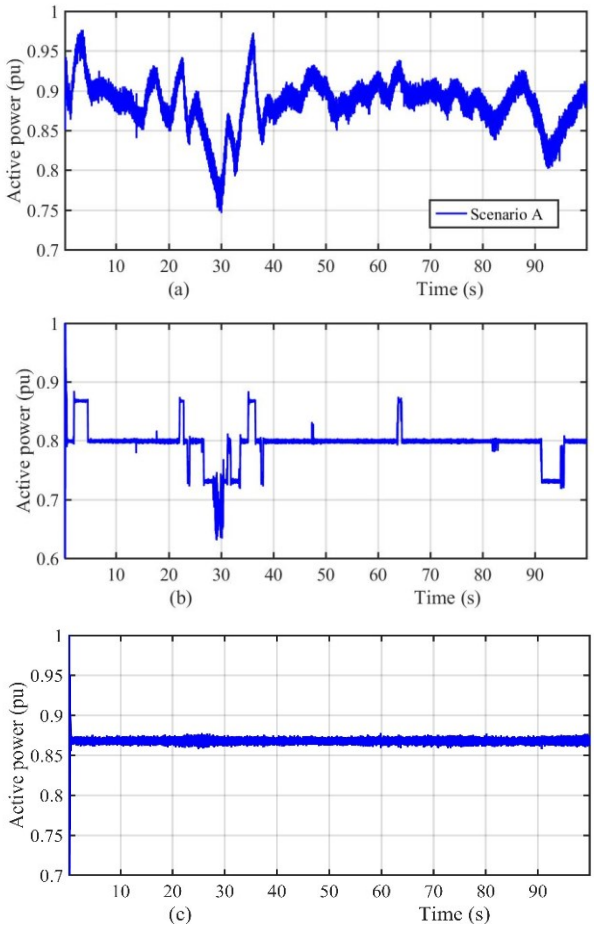


Fig. 7. WPP output power for three scenarios under variable wind speed conditions (a) Scenario A, (b) Scenario B and, (c) Scenario C

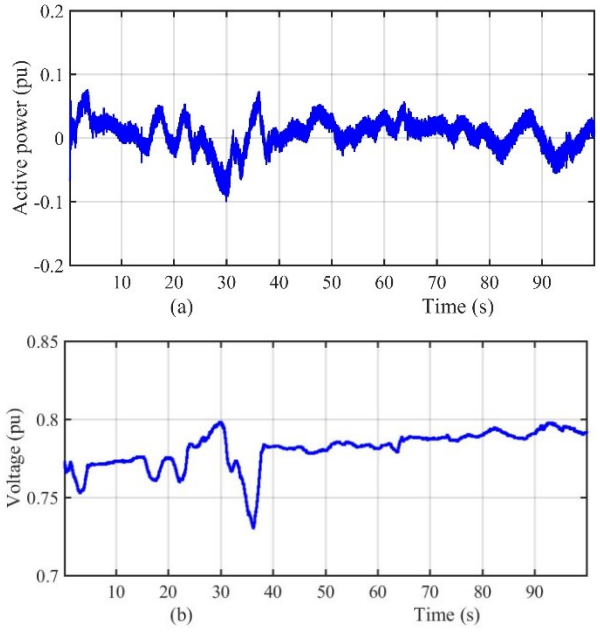


Fig. 8. Super-capacitor (a) output power and, (b) voltage

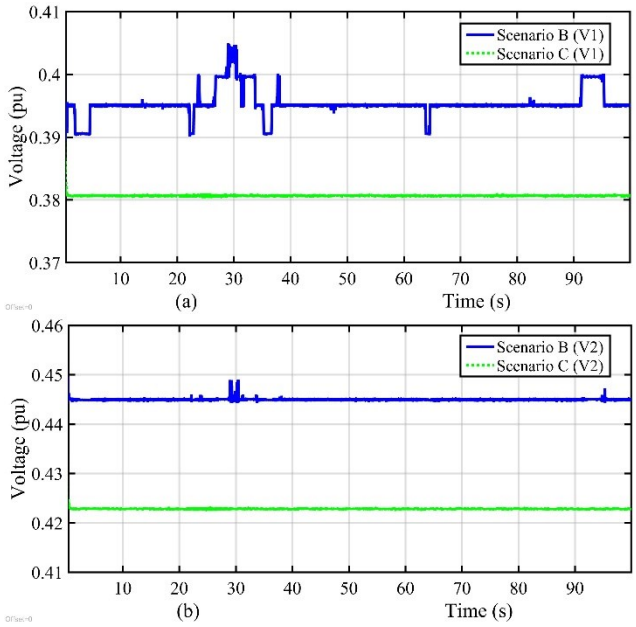


Fig. 9. Voltage injected by (a) inductive SEC branch and, (b) capacitive SEC branch

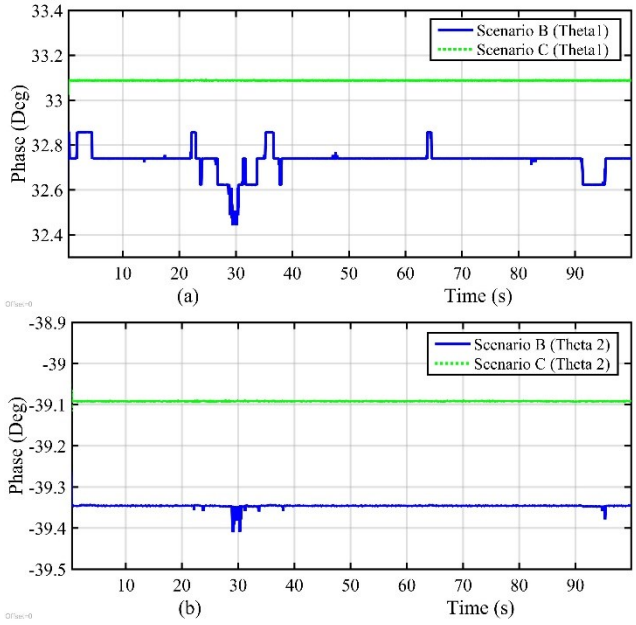


Fig. 10. Voltage phase angle (a) inductive branch and, (b) capacitive branch

### B. Enhancing LVRT Capability

In this section, a 3LG fault is simulated on transmission line to evaluate the capability of the UIPC/ESS for enhancing the LVRT capability of WPP. Fault occurs at *t= 5s* and lasts for *150 ms*. Wind speed is considered to be *15m/s* and constant. Fig. 11(a) shows the active power of the WPP under this condition for all scenarios. In scenario A, the WPP active power drops to zero, approximately. In scenario B, the WPP active power reduces to 0.5 pu at fault instant and raises to 1.6 pu after fault clearance. However, by using the UIPC/ESS in scenario C, it has lower oscillation and power drop compared with scenario B. Fig. 11(b) shows the reactive power in this condition for all scenarios. It can be seen from this figure that the WPP absorbs -2.6 pu reactive power from grid in scenario A. However, in scenarios B and C, the UIPC injects 0.5 and 0.9 pu reactive power to enhance LVRT capability of the WPP, respectively.

Fig. 12(a) shows the rms value of rotor current for all scenarios. As shown in this figure, the rotor current raises to 1.3 pu in scenario A. However, in other two scenarios, the rotor current is effectively limited to 1.2 pu and 0.95 pu, respectively. Fig. 12(b) shows the DC link voltage for all scenarios. It can be seen that by using the UIPC/ESS, the DC link voltage remains constant during fault period. Fig. 12(c) shows the WPP terminal voltage for all scenarios. In scenario A, the terminal voltage falls to 0.2 pu. However, the terminal voltage is 0.8pu and 0.92pu for scenarios B and C under this condition.

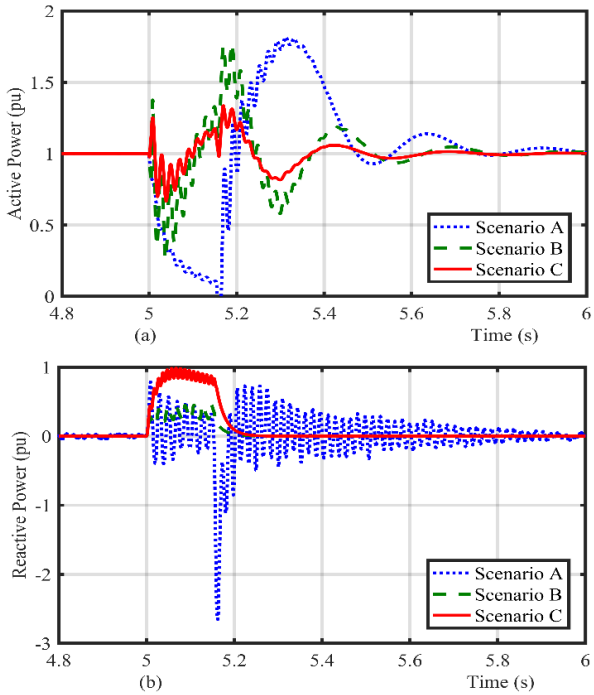


Fig. 11: UIPC/ESS performance under 3LG fault, (a) active power and, (b) reactive power

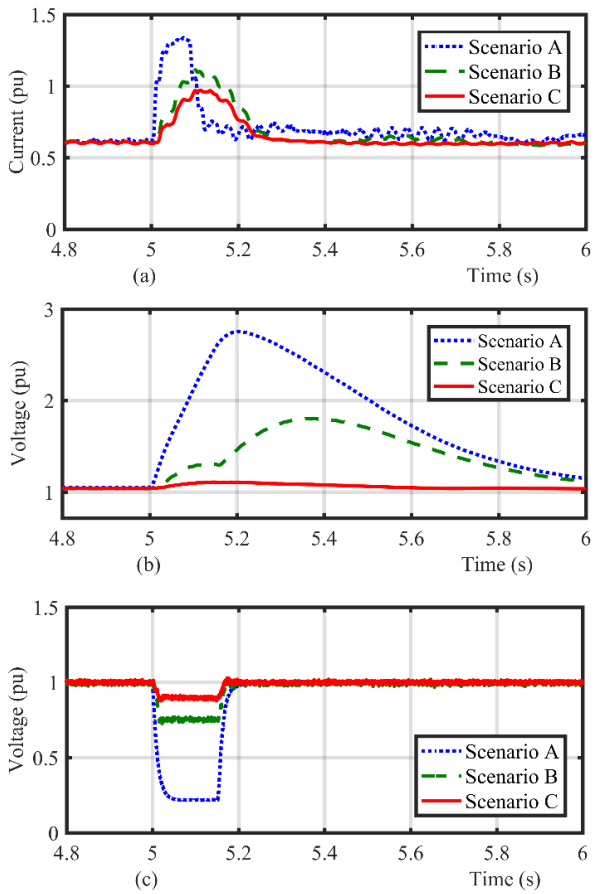


Fig. 12: UIPC/ESS performance under 3LG fault, (a) Rotor current, (b) DC link voltage, (c) terminal voltage

## VI. Conclusion

In this paper is presented an output power smoothing scheme for WPPs, based on UIPC equipped with SC-based ESS. To achieve this, a supervisory control has been designed to generate the reference power for the UIPC and ESS. Additionally, its performance is compared to the case of utilizing UIPC without ESS under variable wind speed in normal and 3LG fault conditions.

Simulation results demonstrate that using the UIPC/ESS, the output power of WPP is effectively smoothened. Moreover, integration of the ESS to the UIPC increases the UIPC capability to enhance the LVRT performance of WPP.

## References

[1] G. W. E. Council, "Global Wind 2015 Report: Annual Market Update," Global Wind Energy Council (GWEC), Brussels, Belgium, 2016.

[2] L. Qu and W. Qiao, "Constant power control of DFIG wind turbines with supercapacitor energy storage," IEEE Transactions on Industry Applications, vol. 47, no. 1, pp. 359-367, 2011.

[3] A. M. Howlader, N. Urasaki, A. Yona, T. Senjyu, and A. Y. Saber, "A review of output power smoothing methods for wind energy conversion systems," Renewable and Sustainable Energy Reviews, vol. 26, pp. 135-146, 2013.

[4] T. Ikegami, C. T. Urabe, T. Saitou, and K. Ogimoto, "Numerical definitions of wind power output fluctuations for power system operations," Renewable Energy, vol. 115, pp. 6-15, 2018.

[5] F. Jia, X. Cai, and Z. Li, "Frequency-Distinct Control of Wind Energy Conversion System Featuring Smooth and Productive Power Output," IEEE ACCESS, vol. 6, pp. 16746-16754, 2018.

[6] A. M. Howlader, N. Urasaki, A. Yona, T. Senjyu, A. Y. Saber," A review of output power smoothing methods for wind energy conversion systems," Renewable and Sustainable Energy Reviews, Vol. 26, pp.135-146, Oct. 2013.

[7] S. G. Varzaneh, G. Gharehpetian, and M. Abedi, "Output power smoothing of variable speed wind farms using rotor-inertia," Electric Power Systems Research, vol. 116, pp. 208-217, 2014.

[8] X. Zhao, Z. Yan, Y. Xue, and X.-P. Zhang, "Wind power smoothing by controlling the inertial energy of turbines with optimized energy yield," IEEE Access, vol. 5, pp. 23374-23382, 2017.

[9] M. Chowdhury, N. Hosseinzadeh, and W. Shen, "Fuzzy logic systems for pitch angle controller for smoothing wind power fluctuations during below rated wind incidents," in PowerTech, 2011 IEEE Trondheim, 2011, pp. 1-7: IEEE.

[10] M. Chowdhury, N. Hosseinzadeh, and W. Shen, "Smoothing wind power fluctuations by fuzzy logic pitch angle controller," Renewable Energy, vol. 38, no. 1, pp. 224-233, 2012.

[11] A. Uehara et al., "A coordinated control method to smooth wind power fluctuations of a PMSG-based WECS," IEEE Transactions on Energy Conversion, vol. 26, no. 2, pp. 550-558, 2011.

[12] S. Nomura, Y. Ohata, T. Hagita, H. Tsutsui, S. Tsuji-Iio, and R. Shimada, "Wind farms linked by SMES systems," IEEE Transactions on Applied Superconductivity, vol. 15, no. 2, pp. 1951-1954, 2005.

[13] M. Sheikh, S. Muyeen, R. Takahashi, and J. Tamura, "Smoothing control of wind generator output fluctuations by PWM voltage source converter and chopper controlled SMES," European Transactions on Electrical Power, vol. 21, no. 1, pp. 680-697, 2011.

[14] T. Kinjo, T. Senjyu, N. Urasaki, and H. Fujita, "Output levelling of renewable energy by electric double-layer capacitor applied for energy storage system," IEEE Transactions on Energy conversion, vol. 21, no. 1, pp. 221-227, 2006.

[15] C. Abbey and G. Joos, "Supercapacitor energy storage for wind energy applications," IEEE Transactions on Industry Applications, vol. 43, no. 3, pp. 769-776, 2007.

[16] R. Cárdenas, R. Peña, G. Asher, and J. Clare, "Power smoothing in wind generation systems using a sensorless vector controlled induction machine driving a flywheel," IEEE Transactions on Energy Conversion, vol. 19, no. 1, pp. 206-216, 2004.

[17] M. Khalid and A. Savkin, "A model predictive control approach to the problem of wind power smoothing with controlled battery storage," Renewable Energy, vol. 35, no. 7, pp. 1520-1526, 2010.

[18] M. T. Zareifard, A. V. Savkin , "Model predictive control for wind power generation smoothing with controlled battery storage," 2015 10th Asian Control Conference (ASCC) 2015 10th Asian Control Conference (ASCC), IEEE, Kota Kinabalu, Malaysia, September 2015

[19] S. Teleke, M. E. Baran, A. Q. Huang, S. Bhattacharya, and L. Anderson, "Control strategies for battery energy storage for wind farm dispatching," IEEE Transactions on Energy Conversion, vol. 24, no. 3, pp. 725-732, 2009.

[20] M. Beza and M. Bongiorno, "An adaptive power oscillation damping controller by STATCOM with energy storage," IEEE Trans. Power Syst., vol. 30, no. 1, pp. 484-493, 2015.

[21] A. Kanchanaharuthai, V. Chankong, and K. A. Loparo, "Transient stability and voltage regulation in multimachine power systems vis-à-vis STATCOM and battery energy storage," IEEE Trans. Power Syst, vol. 30, no. 5, pp. 2404-2416, 2015.

[22] Q. Wang and S. Choi, "The design of battery energy storage system in a unified power-flow control scheme," IEEE Transactions on Power Delivery, vol. 23, no. 2, pp. 1015-1024, 2008.

[23] Bidadfar, A. et.al, "Power swings damping improvement by control of UPFC and SMES based on direct Lyapunov method application" IEEE Power and Energy Society General Meeting ,2008, pp: 1 – 7

[24] T. Mahto, V. Mukherjee," Frequency stabilisation of a hybrid two-area power system by a novel quasi-oppositional harmony search algorithm'' IET Generation, Transmission & Distribution, Vol. 9 , No. 15, pp. 2167 – 2179, Nov. 2015

[25] M. Firouzi, G. B. Gharehpetian, and B. Mozafari, "Power-flow control and short-circuit current limitation of wind farms using unified interphase power controller," IEEE Transactions on Power Delivery, vol. 32, no. 1, pp. 62-71, 2017.

[26] J. Brochu, F. Beauregard, J. Lemay, G. Morin, P. Pelletier, and R. Thallam, "Application of the interphase power controller technology for transmission line power flow control," IEEE transactions on power delivery, vol. 12, no. 2, pp. 888-894, 1997.

[27] M. Farmad ; S. Farhangi ; S. Afsharnia ; G.B. Gharehpetian, "Modelling and simulation of voltage source converter-based interphase power controller as fault-current limiter and power flow controller," IET Generation, Transmission & Distribution, vol. 11, no. 5, pp. 1132 - 1140, 2011

[28] J. Pourhossein, G. Gharehpetian, and S. Fathi, "Unified interphase power controller (UIPC) modeling and its comparison with IPC and UPFC," IEEE transactions on power delivery, vol. 27, no. 4, pp. 1956-1963, 2012.

[29] M. Alizadeh, N. Khodabakhshi-Javinani, G. Gharehpetian, and H. Askarian-Abyaneh, "Performance analysis of distance relay in presence of unified interphase power controller and voltage-source converters-based interphase power controller," IET Generation, Transmission & Distribution, Vol. 9 , No. 13, pp. 1642–1651, Sep. 2015

[30] M. Zolfaghari, M. Abedi, and G. B. Gharehpetian, "Power Flow Control of Interconnected AC-DC Microgrids in Grid-Connected Hybrid Microgrids Using Modified UIPC," IEEE Transactions on Smart Grid, IEEE Transactions on Energy Conversion, Vol. 10, No. 6, pp. 6298 - 6307, Nov. 2019.

[31] M. Firouzi, G. B. Gharehpetian, and S. B. Mozafari, "Application of UIPC to improve power system stability and LVRT capability of SCIG-based wind farms," IET Generation, Transmission & Distribution, vol. 11, no. 9, pp. 2314-2322, 2017.

[32] M. Firouzi, G. B. Gharehpetian, and Y. Salami, "Active and reactive power control of wind farm for enhancement transient stability of multi-machine power system using UIPC," IET Renewable Power Generation, vol. 11, no. 8, pp. 1246-1252, 2017.

[33] Y. Errami, M. Ouassaid, and M. Maaroufi, "Optimal power control strategy of maximizing wind energy tracking and different operating conditions for permanent magnet synchronous generator wind farm," Energy Procedia, vol. 74, pp. 477-490, 2015.

[34] L. Fernandez, C. Garcia, and F. Jurado "Equivalent model of wind farms by using aggregated wind turbines and equivalent winds," Energy Covers Maneg, Vol. 50, pp. 691–704, 2009.

[35] M. Firouzi and G. B. Gharehpetian, "LVRT Performance Enhancement of DFIG-Based Wind Farms by Capacitive Bridge-Type Fault Current Limiter," IEEE Transactions on Energy Conversion, Vol. 9, No. 3, pp. 1118–1125, 2018.